Multi-temporal NDVI Change Patterns and Global Land Cover Dynamics

Jeong-Chang Seong[1]

다중시기 NDVI 변화 패턴과 토지 피복상태의 변화에 관한 연구

성 정 창[1]

ABSTRACT

Average annual NDVI values from the NOAA/NASA Pathfinder AVHRR Land Data Sets from 1982 to 1994 showed comprehensive systematic displacement patterns in Asia. Inter-annual growing season data, however, did not show such systematic patterns. The most likely cause for the abrupt displacements, which appear especially in 1982, 1989 and 1990, may be changes in satellite sensors, although global warming, El Niño-Southern Oscillation events, changes in processing algorithms, and changes in land-use patterns in various parts of Asia may also play some role. The results suggest that researchers must be extremely careful in their inter-annual global change research, since direct use of the raw data could cause unexpected results. Growing-season NDVI shows decreases throughout most of Southeast Asia and modest gains in northern China and some parts in India, which could be related to land-use and land-cover changes.

KEYWORDS : Global Land Cover, Multi-temporal Approach, Asia, NDVI

요 약

이 연구에서는 NOAA/NASA Pathfinder AVHRR Land Data Sets를 이용하여 시계열 NDVI 자료를 분석하였다. 1982년부터 1994년까지의 자료를 분석한 결과, 연평균 NDVI의 경우, 1982년, 1989년 및 1990년의 자료에서 심각한 계통적 편차가 나타났다. 이 연구에서는 엘니뇨와 위성 센서, 위성자료 처리 알고리듬 및 지표피복의 변화를 통하여 어느 정도의 계통적 편차를 설명할 수 있었다. 한편 식물 성장기의 자료를 이용한 연구기간 동안의 NDVI 변화 추세는 아시아 지역의 토지피복 변화와 많은 관련이 있는 것으로 나타났다.

주요어 : 지구토지피복, 다중시기 접근, 아시아, NDVI

2000년 9월 8일 접수 Received on September 8, 2000
1 Dept. of Geography, Northern Michigan Univ., Marquette, MI, USA (jseong@nmu.edu)

NDVI and Land Cover

As more and more remotely sensed data become available, many researchers are interested in the multi-temporal dynamics of land cover features. Unlike multi-spectral land cover characterizations, multi-temporal approaches provide unique research topics and methods. Sometimes, the distinction between the two approaches is not clear. For instance, multi-spectral approaches have also used multi-temporal imagery in many cases, such as seasonal images to determine ground features showing similar reflectance characteristics in one season but different in another. In order to avoid ambiguity in the terminology for multi-temporal images in this study, 'multi-temporal' will be used to denote a set of images consisting of regularly time-sampled subset images, where the regularity assures that the sample period is shorter than the major phenological change periods occurring to the image features of interest.

Because multi-temporal data are usually voluminous, the normalized difference vegetation index(NDVI) has been considered to be a meaningful data reduction method for multi-temporal land cover monitoring. The NDVI is calculated using the red and infrared bands from a multi-spectral image: NDVI = [Infrared - Red] / [Infrared + Red] (Tucker, 1979; Tarpley et al., 1984; Holben, 1986). Although claims of relationships to 'green leaf biomass' and standing biomass in general are exaggerated, especially above leaf area index (LAI) of about 3, annually integrated NDVI is known to be an indicator of annual primary production(Goward et al., 1985; Box et al., 1989). For the Advanced Very High Resolution Radiometer(AVHRR), the red-band wavelength ranges from 0.58 to 0.68 Φm, where chlorophyll causes considerable absorption of incoming radiation. The near-infrared wavelength ranges from 0.725 to 1.10 Φm, where spongy mesophyll leaf structure leads to considerable reflectance(Agbu and James, 1994). Research has shown that the NDVI is closely related to some geophysical parameters. One of the distinguishing contributions of multi-temporal NDVI is its ability to characterize land cover dynamics at global or regional scale, which has been almost impossible with the traditional spectral approaches based on one or only a few scenes. Especially, with coarse-resolution AVHRR products covering the whole world, the multi-temporal NDVI images have allowed inter-annual monitoring of land cover dynamics. Even though there are many problems in the use of AVHRR NDVI images, many researchers retrieved the main features of land-cover dynamics using phenological and radiometric reflectance characteristics, because NDVI profiles are closely related at least to pheno-physiognomic vegetation types.

Research using NDVI has mostly dealt with relatively short periods. For long-term inter-annual land cover studies, it is important to know the inter-annual variability of the NDVI profiles, because the NDVI profiles are affected by climate change, land use change, sensor characteristics, etc. Unlike short-term research, inter-annual research involves general problems of long-term multi-temporal analysis as well as general land cover changes. This research investigates relatively long-term multi-temporal, regional NDVI change patterns in Asia, and their implications for global study of land cover change. NDVI-related research trends for

characterizing global land cover dynamics will be reviewed in NDVI Research Trend. Data processing procedures and problems of integrated contaminated pixels are described in Methodology. Multi-temporal NDVI Change Pattern shows annual and growing-season NDVI dynamics. Discussion and Conclusion summarize the implications for a global land cover study.

NDVI Research Trend

Researches have shown that NDVI is related to various geophysical parameters. The NDVI has been interpreted as an index of photosynthetic capacity, by which higher NDVI values indicate greater photosynthetic activity (Sellers, 1985). The relationship is especially apparent between annually integrated NDVI and annual net primary production, especially over larger areas(Goward et al., 1985; Box et al., 1989; Prince, 1991; Box and Bai, 1993; Prince and Goward, 1995). On the other hand, the NDVI may also be an index of climatic factors such as actual evapotranspiration(Box et al., 1989) and soil moisture fraction. Cihlar et al. (1991) argued that growing-season NDVI trajectories in Canada(climates with little summer water stress) are most similar to potential evapotranspiration(PET) curves and that the correlation between NDVI and actual evapotranspiration(AET) is high, especially when AET approaches PET rates.

As a multi-temporal approach, the use of temporal NDVI profiles can be grouped into five categories. The first is direct use of the temporal profile itself, for example use of seasonal NDVI fluctuations to show dramatic changes in surface greenness over a large area(e.g. Eidenshink, 1992). The second use involves relating temporal profiles to environmental variables. For example, Malingreau(1986) identified several distinctive temporal NDVI development curves for various environmental zones in Asia and showed the impact of the 1982-1983 drought related to a strong El Niño-Southern Oscillation(ENSO) event. The third use involves development of land-cover classification maps. Based on the 1990-1992 NDVI profile for each land cover type, Achard and Estreguil(1995) classified forest types in Southeast Asia using the unsupervised classification method. Zhu and Evans(1994) also classified forest types in the United States using AVHRR data and the unsupervised classification method. The fourth use involves the metrics of the temporal development curves in order to identify ground-cover characteristics. For example, Defries et al.(1995) used 16 metrics from the NDVI profile and the temperature bands to discriminate land cover types and to compare with the result of a maximum-likelihood classification method. The last use involves the temporal profiles as base data for developing a secondary index. This can be considered adata reduction method. Principal components analysis is used frequently for this purpose. For example, Eastman and Fulk(1993) identified eight principal components from multi-temporal NDVI images. Cicone and Olsenholler(1997) recently used principal components analysis to summarize some aspects of Asian vegetation. This was done by using the Difference Vegetation Index derived from 1km AVHRR data for 1992~1993 to characterize cumulative greenness, summer greenness, early-season greenness increase, and number of greenness peaks as principal components 1 to 4 respectively.

Methodology

AVHRR data have frequently been used for global or regional-scale multi-temporal analysis because of the relatively short satellite return period and the temporal and spatial comprehensiveness of the data. Since the raw AVHRR data are contaminated by clouds, varying sun angle, and other geometric and atmospheric factors, they are composited to make more enhanced images(cf. Holben, 1986). In this study, the Pathfinder AVHRR 8km Land(PAL) Data Sets for 1982-1994 were used(see Agbu and James, 1994). Monthly maximum-value composite images were created using the original 10-day PAL data that were composited from the 4 km Global Area Coverage(GAC) 1B data.

A vector boundary layer from the Global Resource Information Database(GRID) for 1992 was re-projected to the Goode Homolosine projection(Steinwand, 1994) and rasterized to create an index map of political boundaries. For China and India, the provincial boundaries were used in order to balance the size of these large countries with the smaller ones. Annual regional statistics were calculated from the monthly images and the political boundary map. In addition, growing-season images covering the period from June through August were analyzed to investigate inter-annual variance in growing-season NDVI. After analyzing the statistics, NDVI trends were calculated using linear regression. Finally, the regional trend was mapped to show spatial patterns using Jenks' natural-break classification algorithm(Jenks and Caspall, 1971).

Valid NDVI values range from -1 to +1, but only positive values show surface greenness. In order to calculate annual statistics, only those pixels were used which had no bad values on any image. Four statistics were calculated: annual mean over all positive NDVI values, annual mean for positive and negative NDVI values, growing-season mean for positive NDVI values, and growing-season mean for positive and negative NDVI values. After visual screening of all images, it appeared that unscaled PAL values over about 216(scaled: 0.704) and under about 100(scaled: -0.144) showed little relationship to ground features. Thus these extreme values were excluded. Other invalid pixel values were indicated by a Cloud Cover(CLAVR) flag, with integer values ranging from 12 to 30, and a Quality Control flag, with integer values less than 5. Only the remaining, valid pixels were used for monthly maximum NDVI compositing. Monthly composite images were then prepared using the maximum-value compositing method. Finally, average NDVI values were calculated in order to standardize(normalize) for the different number of pixels in each country. Four average values were calculated: averages for positive NDVI values for 12 months(January to December), for all NDVI values for 12 months, for positive NDVI values during the growing season(3 months: June, July and August), and for all NDVI values during the growing season.

Multi-temporal NDVI Change Pattern

Temporal change patterns for positive NDVI values were not much different from those for all(positive and negative) NDVI values. They were almost identical, which meant that negative NDVI values did not significantly affect

the monthly and annual NDVI patterns. Therefore, only the positive NDVI change patterns were analyzed further.

Figure 1 shows the changes in annual average NDVI. The average values were calculated from the twelve monthly images over the 12-year period. The figure shows that Mongolia has the lowest average NDVI throughout the year and Laos the highest. The average NDVI values in the other countries range between 0.25 and 0.50. In general, North Korea, India and Bangladesh show relatively low NDVI levels, and Myanmar, Cambodia and Sri Lanka show high NDVI levels.

Figure 1 also clearly shows systematic displacements in 1982, 1989 and 1990, which make the NDVI values for these years higher than for other years. The average differences (over all pixels in the images) are 0.086 between 1982 and 1983, 0.042 between 1988 and 1989, and 0.036 between 1990 and 1991. Lower values are also shown in 1992 and 1993 in many countries. From 1983 to 1988, most profiles do not show dramatic changes but only slight fluctuations. Less vegetated areas, such as Mongolia, Jamu-Kashmir, the Chinese provinces of Inner Mongolia, Xinjiang-Uygur, and Tibet show smaller displacements in 1989 and 1990. There are also distinctive decreasing trends in Bhutan, China, Japan, North Korea, South Korea and Taiwan since 1990, while

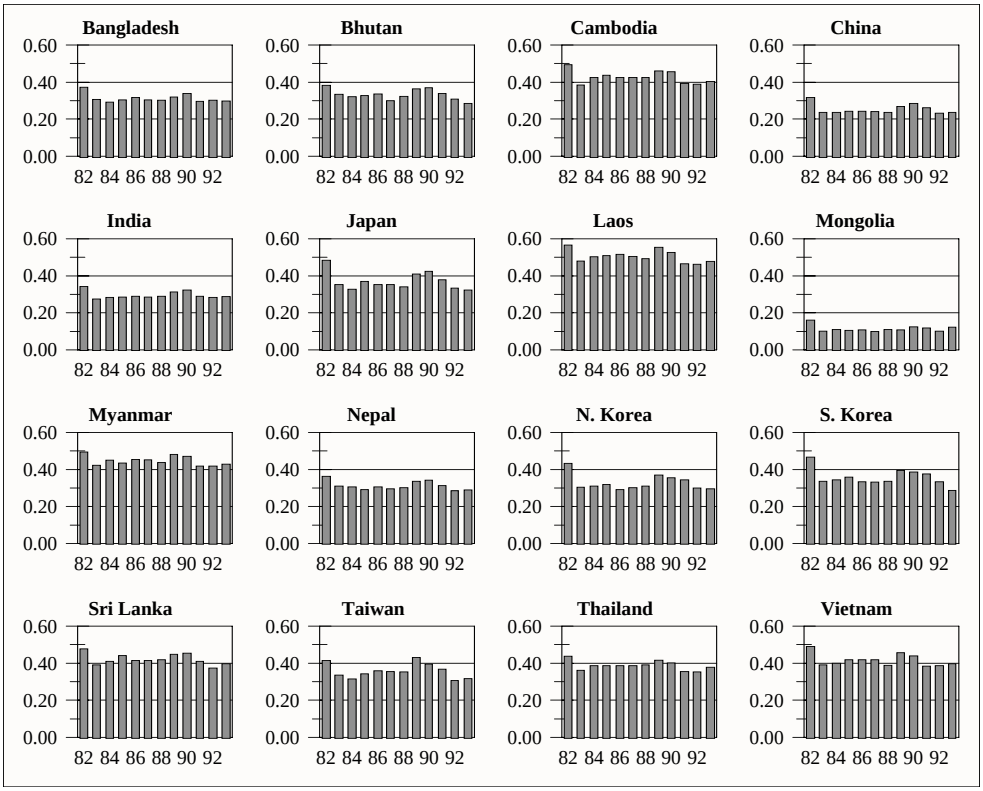

FIGURE 1. Annual average NDVI change in Asia, 1982~1993.

Mongolia, India and Myanmar, on the other hand, show relatively consistent NDVI levels.

Figure 2 shows inter-annual changes in NDVI levels during the growing season (defined as June through August). Some countries, i.e., China, South Korea, Japan, Sri Lanka, Vietnam, Taiwan and North Korea, show systematic changes between 1982 and 1983, but not as high as for the full-year data (Figure 1). Three distinctive groups of countries are apparent in Figure 2: areas with generally low NDVI levels(Mongolia, India, Bhutan, Bangladesh and Nepal), intermediate NDVI levels(Taiwan, Thailand, Myanmar, China, Sri Lanka and Vietnam), and high NDVI levels(Cambodia, South Korea, North Korea and Japan). The low and high groups show somewhat increasing trends, but the intermediate group shows generally decreasing trends. The anomalies of 1989 and 1990 also appear in some countries. The generally slight increasing trends in growing-season NDVI levels correspond to an earlier result showing a slightly increasing inter-annual trend in average growing-season NDVI calculated only from non-interpolated raw NDVI data.

Based on these general NDVI trends, the change patterns of average growing-season NDVI were characterized by linear regression, deleting data for 1982, 1989 and 1990. The results showed inter-annual trends in growing-season NDVI, represented by degree of annual change. Southeast Asian countries (Thailand, Laos, Cambodia and Vietnam),

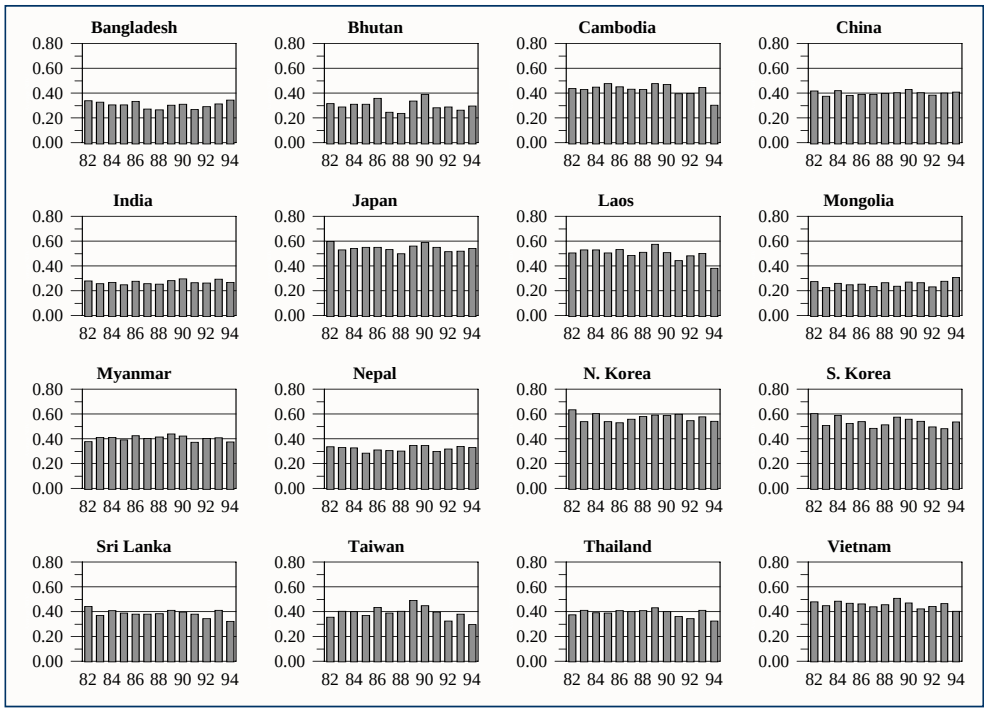

Figure 2. Growing season(June, July and August) average NDVI change in Asia, 1982~1994. This figure covers one more year, 1994, because the Pathfinder AVHRR Land Data Set covers the growing season.

southeastern parts of China(Guangdong and Fujian), Taiwan, and northeastern parts of India(Meghalaya and Mizoram) show strong continuous decreases. Slight decreases appear in Japan, South Korea, some parts of China (Jiangxi, Shanghai and Guizhou), Myanmar, Bhutan and several parts in India(Orissa, Sikkim, Kerala, Goa, Tripura and Nagaland). On the contrary, many parts of northeastern and western China, northern and western India, plus Sri Lanka and Mongolia, show slight NDVI increases. Large increases appear in Hebei(China) and in Bihar, Haryana and Punjab(India). North Korea and many other parts in India and China show consistent patterns.

Discussion

While the multi-spectral approach uses mainly the multi-spectral reflectance characteristics, the multi-temporal approach incorporates multi-temporal phenological characteristics as well as the multi-spectral reflectance characteristics. This requires users of global NDVI data to be more cautious. Based on this study, it appears that the following three issues are important for multi-temporal global studies of land-cover change. First, given the uncertainty of image accuracy, multi-temporal images usually contain more complexity than do multi-spectral images. Different imaging conditions, especially varying atmospheric and climatic conditions, and soil moisture conditions, and different physical sensor characteristics make it more difficult to control or correct various kinds of error. Second, the radiometric normalization(over all images, for all months of all years) becomes a major error source in multi-temporal analyses. Several methods have been suggested for handling this problem(Jensen, 1996), but it is still difficult to standardize multiple images effectively in a single fashion. Third, the multi-temporal approach poses problems of cumulative, compounded contamination. When the bad pixels resulting from bad seasonal scan angle, constant heavy cloud contamination and long-lasting snow cover are collected into one error image, the total contaminated area usually comprises a large portion of the image, which makes it hard to analyze the whole image.

This research clearly shows distinctive systematic displacement patterns in the images for annually integrated NDVI for 1982, 1989 and 1990. These displacements could be attributed to changes in satellite sensors, climate conditions, processing procedures, or land uses. A climatic cause is unlikely, because the displacement appears to be systematic and occurs throughout the study area, in desert, grassland and forest. Climatic factors would not normally affect all areas. An ENSO event, which is associated with droughts and floods in Asia, did occur from the second quarter of 1982 through the third quarter of 1983(Toole and Borges, 1984), coinciding with the systematic displacement in 1982(Figure 2). Other El Niño events occurred from mid-1986 to early 1988 and from mid-1991 through 1993. These events, however, did not coincide with the NDVI increases in 1989 and 1990, and do not seem to have caused systematic displacements. Global surface temperatures have increased about 0.3E to 0.6EC since the 19th Century (e.g. Nicholls et al., 1996), and recent warming has been greatest between 40E and 70E latitude in the Northern Hemisphere. Temperatures in the Northern Hemisphere are

thought to have increased about 0.3EC since 1983(e.g. Jones and Briffa, 1992; NSTC, 1997), with small dips in 1982, 1984~1985 and 1992~1993. The NSTC report indicated in particular that the warmest year during the study period of 1983~1994 was 1990. In this context, ENSO and global warming may contribute to the systematic NDVI change to some degree, but it is hard to identify them as main causal factors for systematic NDVI anomalies.

Artifacts, such as change of satellite sensor and errors or changes in data processing, are more likely to cause systematic differences. According to James and Kalluri(1994), there were marked differences in the stability and precision of the three AVHRR sensors launched on 23 June 1981(NOAA7), 12 December 1984 (NOAA9) and 24 September 1988(NOAA11). The annual systematic displacements coincide

TABLE 1. AVHRR-PAL processing corrections and effects on NDVI(Agbu and James, 1994; Kalluri, 1996).

Errata	Correction	Description	Effect to NDVI
Relative azimuth representation (1994)	Yes	The original relative azimuth value(Solar azimuth minus sensor azimuth) at nadir was set to zero, but changed th 'missing'. As the result, no NDVI at nadir is calculated or binned.	Quite minor effect to NDVIl
Error in the CLAVR algorithm(1994)	Yes	A coding error brought that the Reflectance Gross Cloud Test rarely flagged data as cloudy. It was fixed.	None. Users are to be cautious about using the CLAVR layer.
Error in the thermal calibration algorithm(1994)	Yes	Incorrect application of 'negative radiation from space'. Changes on average in channel 4 was 0.71K and in channel 5 0.41K.	No effect on NDVI, visible and geometry layers.
Change of ozone input data in the atmospheric correction algorithm(1994)	Yes	Change to using daily ozone data instead of using only the first day data of the month from the Total Ozone Mapping Spectrometer(TOMS).	The overall affect is small enough that inter-annual comparisons can still made.
Handling quality control flags in the compositing algorithm(1994)	Yes	The original NOAA quality control flags that indicate incorrect 효 a number of conditions were filtered out.	Composite data sets are affected.
Computation of Solar Zenith Angles(1996)	No	The error in th Solar Zenith Angle varies systematically with time and geographical location. The errors are smaller in the recent data(e.g., ±2 degrees in the 1992 data) and larger in the earlier data(e.g., ±7 degrees in the 1982 data).	Channel 1 and 2, reflectances, NDVI, CLAVR flags and the relative azimuth angles are affected. The differences in NDVI obtained with accurate and inaccurate Solar Zenith Angle, however, anr negligible.

temporally with the early data from the NOAA7 and NOAA11. The decreasing trends since 1990 could be due to sensor degradation. It is interesting, though, that there is little if any such effect during the period from 1984 to 1987 which could be attributable to sensor degradation.

Changes in coding, calibration and processing algorithms, often due to subsequent finding of new errors(cf. Agbu and James, 1994; Kidwell, 1997), can cause NDVI anomalies. Table 1 shows the changes applied to the AVHRR data prior to their release in 1994. Even afterward, in 1996, an error in estimation of the solar azimuth was found. Land-use changes can also be considered, but they would not likely bring about the comprehensive annual change patterns because the displacements occur in all countries. In this context, it seems that all four factors may contribute to some degree but that different sensors and data processing methods may be the main causes of the systematic displacement patterns in annually integrated NDVI.

In contrast to the patterns of comprehensive systematic change in annually integrated NDVI, growing-season NDVI trends show geographic patterns: decreases in most Southeast Asian countries, in southeastern China, and in Japan and Korea, but increases in northern China, Mongolia and some parts in India. These patterns could be related to changes in global climate or in land-use patterns or both. The pattern of greatest warming at 40-70EN(cf. Nicholls et al., 1996) does not disagree with the pattern of increasing NDVI in this area, but increases also occur in some areas of India. The systematic changes shown in the annual NDVI do not appear as distinctly in the growing-season patterns but may still be there to some degree. This suggests that one must be especially careful when using multi-temporal data. It may be particularly risky to attempt to relate multi-annual NDVI data to geophysical parameters(e.g. using NDVI metric indices as indicators of changes in ground features).

Conclusions

This research investigated the characteristics of AVHRR NDVI data-sets for use with inter-annual land cover studies and then analyzed spatio-temporal land cover dynamics in Asia. The results showed systematic displacements in the annual and growing-season multi-year average NDVI in 1982, 1989 and 1990. The anomalies are thought to be due mainly to changes in sensing devices, although processing changes(and perhaps errors), climate change and changes in land use may play some role. In addition, integration of contaminated pixels may cause other problems in large-area multi-temporal studies. In the study of NDVI change over Asia, about 53% of the land area contained at least one bad pixel in the 144 consecutive monthly images. As a solution, linear interpolation was used in this study to patch the bad or missing data. Finally, the growing-season NDVI trends suggested a relationship to global warming in higher latitudes and perhaps to changes in land use in Southeast Asia, southeastern China, Taiwan, Japan and Korea. These results indicate that a great deal of attention must be paid to such overriding influences when one performs multi-annual spatio-temporal analyses. In particular, data characteristics should be thoroughly analyzed beforehand, and raw NDVI data should not be used without prior checks

for systematic trends and discontinuities.

ACKNOWLEDGMENT

Data used in this study include data produced through funding from the Earth Observing System Pathfinder Program of NASA's Mission to Planet Earth in cooperation with the National Oceanic and Atmospheric Administration. These data were provided by the Earth Observing System Data and Information System, Distributed Active Archive Center at Goddard Space Flight Center, which archives, manages, and distributes this data-set. KAGIS

REFERENCES

Achard, F. and C. Estreguil. 1995. Forest classification of southeast Asia using NOAA AVHRR Data. Remote Sensing of Environment 54. 198-208.

Agbu, P.A. and M.E. James. 1994. The NOAA/NASA Pathfinder AVHRR Land Data-Set User's Manual. Goddard Distributed Active Archive Center, NASA, Goddard Space Flight Center, Greenbelt, Maryland.

Box, E.O. and X.M. Bai. 1993. A satellite-based world map of current terrestrial net primary productivity. Seisan-Kenkyu(Tokyo) 45(9):666-672.

Box, E.O., B.N. Holben, and V. Kalb. 1989. Accuracy of the AVHRR vegetation index as a predictor of biomass, primary productivity, and net CO2 flux. Vegetatio 80:71-89.

Cicone, R.C. and J.A. Olsenholler. 1997. A summary of Asian vegetation using annual vegetation dynamic indicators. Geocarto International 12(1):13-25.

Cihlar, J., L. St.-Laurent, and J.A., Dyer. 1991. Relation between the Normalized Difference Vegetation Index and ecological variables. Remote Sensing of Environment 35:279-298.

Defries, R.S., M. Hansen and J.R.G. Townshend. 1995. Global discrimination of land cover types from metrics derived from AVHRR Pathfinder data. Remote Sensing of Environment 54:209-222.

Eastman, J.R and M. Fulk. 1993. Long-sequence time-series evaluation using standardized principal components. Photogrammetric Engineering and Remote Sensing 59(6): 991-996.

Eidenshink, J.C. 1992. The 1990 conterminous U.S. AVHRR data-set. Photogrammetric Engineering and Remote Sensing 58(6): 809-813.

Goward, S.N., C.J. Tucker and D.G. Dye. 1985. North American Vegetation Patterns Observed with the NOAA-7 Advanced Very High Resolution Radiometer. Vegetation 64: 3-14.

Holben, B.N. 1986. Characteristics of maximum-value composite images from temporal AVHRR data. International Journal of Remote Sensing 7(11):1417-1434.

James, M.E. and S.N.V. Kalluri. 1994. The Pathfinder AVHRR land data-set: An improved coarse data set for terrestrial monitoring. International Journal of Remote Sensing 15(17):3347-3363.

Jenks, G.F. and F.G. Caspall. 1971. Error on choropleth maps: definition, measurement, reduction. Annals of Association of American Geographers 61:217-244.

Jensen, J.R. 1996. Introductory Digital Image Processing: A Remote Sensing Perspective. 2nd ed., Prentice Hall, New Jersey.

Jones, P.D. and K.R. Briffa. 1992. Observed surface temperature data. The Holocene 2:165-179.

Kalluri, S.N.V. 1996. Errors in the computation of solar zenith angles in the PAL data-set.

http://daac.gsfc.nasa.gov/CAMPAIGN_DOCS/LAND_BIO/zenith_angle_memo.html.

Kidwell, K.B. 1997. NOAA Polar Orbiter Data Users Guide (TIROS-N, NOAA6, NOAA7, NOAA8, NOAA9, NOAA10, NOAA11, NOAA12, NOAA13 and NOAA14). National Oceanic and Atmospheric Administration, National Environmental Satellite, Data, and Information Service (NESDIS).

Malingreau, J.P. 1986. Global vegetation dynamics: Satellite observations over Asia. International Journal of Remote Sensing 7(9):1121-1146.

Nicholls, N., G.V. Gruza, J. Jouzel, T.R. Karl, L.A. Ogallo, and D.E. Parker. 1996. Observed Climatic Variability and Change. In: Houghton, J.T., Filho, L.G. M., Callender, B.A., Harris, N., Kattenberg, A., and Maskell, K.(Eds.), Climate Change 1995: The Science of Climate Change. The Intergovernmental Panel on Climate Change(IPCC), pp.133-192.

NOAA(National Oceanic and Atmospheric Administration). 1994. El Niño and Climate Prediction. Reports to the Nation on Our Changing Planet.

NSTC(National Science and Technology Council). 1997. U.S. Global Change Research Report: Our changing planet, An investment in science for the nation's future.

Prince, S.D. 1991. Satellite remote sensing of primary production: Comparison of results for Sahelian Grasslands 19811988. International Journal of Remote Sensing 12(6):1301-1311.

Prince, S.D. and S.N. Goward. 1995. Global primary production: A remote-sensing approach. Journal of Biogeography 22:815-835.

Roy, N.S. 1998. ENSO and the Asian Monsoon. The ENSO Signal, Issue 9.

Seong, J.C. 1998. Estimation of General Systematic Errors Between Two Multi-Temporal Global NDVI Composite Images using the Polynomial Curve Fitting Method. ASPRS-RTI 1998 Annual Conference Proceedings, pp.1021-1029.

Sellers, P.J. 1985. Canopy reflectance, photosynthesis and transpiration. International Journal of Remote Sensing 6:1335-1372.

Steinwand, D.R. 1994. Mapping raster imagery to the Interrupted Goode Homolosine projection. International Journal of Remote Sensing 15(17):3463-3471.

Tarpley, J.D., S.R. Schneider and R.L. Money. 1984. Global vegetation indices from the NOAA7 Meteorological Satellite. Journal of Climate and Applied Meteorology 23:491-494.

Toole, J.M. and M.D. Borges. 1984. Observations of horizontal velocities and vertical displacements in the equatorial Pacific Ocean associated with the early stages of the 1982/83 El Niño. Journal of Physical Oceanography 14:948-959.

Tucker, C.J. 1979. Red and photographic infra-red linear combinations for monitoring vegetation. Remote Sensing of Environment 8:127-150.

Zhu, Z. and D.L. Evans. 1994. U.S. Forest Types and predicted percent forest cover from AVHRR data. Photogrammetric Engineering and Remote Sensing 60(5): 525-531.